# Self-Diagnosis of Acoustic Emission Sensors: Electromechanical Impedance-Based Damage Detection

CHRISTOPHER REINHARDT, ADELMO FERNANDES, MATTHIAS MERZKIRCH, MARKUS G. R. SAUSE and INKA MUELLER

**ABSTRACT**

The reliability and functionality of Acoustic Emission (AE) sensors is essential for their role in non-destructive testing (NDT) and structural health monitoring (SHM) systems. Conventional field-verification methods, such as the pencil lead break test (Hsu-Nielsen source), require manual interaction and are susceptible to external influences from the test structure. Furthermore, human interaction in close proximity to the sensor location requires a considerable effort when monitoring structures such as bridges or wind turbines. These shortcomings often necessitate additional verification under laboratory conditions, thereby underscoring the requirement for a more efficient and reliable approach to the verification of AE sensor performance in the field. A promising solution is the analysis of the electromechanical impedance (EMI) spectrum of AE sensors. This method facilitates remote and automated self-diagnosis by capturing the mechanical and electrical characteristics of the sensor, as well as its interactions with the coupling layer and surrounding structure.

This paper presents the experimental investigation of the detection of mechanical damage in AE sensors using the EMI spectrum. The damage was induced systematically by controlled drop-down tests, which simulated realistic degradation scenarios. The experimental results are further validated by comparison with an established wave-based verification setup described in the guideline for the verification of sensors and their coupling in laboratories by the German society for non-destructive testing, which is a widely accepted standard for AE sensor verification under laboratory conditions. The comparison of EMI-based self-diagnosis with the wave-based SE02 verification method demonstrates that the EMI is capable of reliably detecting sensor damage. This provides evidence that the EMI-based self-diagnosis is a viable alternative to traditional manual and laboratory-based methods. Moreover, this approach offers several significant advantages, including automation, reduced reliance on human input, and suitability for deployment in field conditions. By addressing common damage scenarios, such as mechanical degradation from impacts, this work contributes to the development of robust self-diagnosis capabilities for AE sensors.

Christopher Reinhardt, Inka Mueller, Bochum University of Applied Sciences, Germany
Adelmo Fernandes, Matthias Merzkirch, Markus G. R. Sause, University of Augsburg, Germany

## INTRODUCTION

The use of acoustic emission (AE) testing is widely employed in non-destructive testing (NDT) and structural health monitoring (SHM) as it is a powerful technique to detect and analyze transient elastic waves generated by structural degradation mechanisms such as crack formation or impact events. The physical conversion of the elastic waves is mostly realized by a piezoelectric element in the AE sensor [1]. Given the increasing utilization of AE systems for long-term monitoring of large-scale and safety-critical structures, such as bridges, wind turbines, and pressure vessels, the reliability and functionality of AE sensors are critical to ensuring the accuracy and validity of the collected data. Undetected damages in the sensors can result in false-negative assessments of structural integrity, which potentially lead to hazardous outcomes.

Established field-verification techniques, such as the pencil lead break test (also known as the Hsu-Nielsen source), provide a basic assessment of the sensor's performance in-situ. However, this method requires physical access to the sensor, human interaction and is sensitive to external influences from the test structure. Therefore, an additional verification under laboratory conditions is often required and an automated, remote verification of the sensor's performance is not possible. With the verification in the laboratory, more advanced diagnostic methods are available, including face-to-face coupling of AE sensors with ultrasonic transducers to generate a defined sensitivity spectrum [2, 3] or coupling to a free vibrating aluminum block excited by a piezoelectric actuator to compare the response against established reference baselines [4, 5]. The verification principle of the latter is also realized within a mobile verification device using an aluminum plate instead of a block [6].

A promising approach for AE sensor verification is the analysis of the electromechanical impedance (EMI) spectrum, a complex, frequency-dependent quantity that reflects the interaction between the piezoelectric element, the sensor's casing, the coupling interface, and the structure. As such, the EMI spectrum offers valuable insight into changes in the sensor's physical state. Furthermore, this approach is an established verification method for piezoelectric wafer active sensors (PWAS) used for guided waves [7–9]. Recent studies have demonstrated the feasibility of EMI-based self-diagnosis through laboratory tests on 29 used sensors with unknown damage states [10]. Follow-up research explored the influence of different coupling conditions and structural parameters [11] and specific damage mechanisms, such as thermal degradation of the adhesive layer [12]. Across these studies, features like correlation coefficient (CC), root-mean-square (RMS), eigenfrequency (EF) shifts, sum of peak amplitudes, and slope of the linear section at lower frequencies were used to assess the sensor's condition and parameter influences.

This work presents the results of an experimental study on the detection of mechanical damage in AE sensors using their EMI spectrum. Mechanical degradation was systematically induced through controlled drop tests to replicate realistic damage scenarios. The EMI-based damage detection is validated against a wave-based verification setup, in accordance with SE02 by the DGZfP [4], an established laboratory standard for AE sensor verification, located at the University of Augsburg. The comparison enables a direct assessment of the EMI method's reliability in identifying sensor damage. It highlights the potential of EMI-based self-diagnosis as an in-situ alternative to traditional

verification techniques.

## MATERIAL AND METHODS

Within this work, experimental measurements of the EMI and wave signal after a defined pulse through an aluminum block were used to assess the state of two AE sensors of different type. The sensors were of the type VS150-M and VS30-V manufactured by Vallen Systeme GmbH. The sensors were damaged through controlled drop tests with the experimental setup described in [6]. For the drop test, a steel ball with a weight of $24\,\mathrm{gr}$ fell from a defined height on the side of the sensor. The drop height of the ball started at $150\,\mathrm{mm}$ and was increased by $100\,\mathrm{mm}$ after every third drop. Subsequent to each drop, an EMI measurement and wave-based measurement was conducted and preliminarily evaluated. This provided the opportunity to have a first rough assessment of the sensor's state. Therefore, it was possible to reduce the drop height after first damage was noticeable. This was the case after the second drop from $850\,\mathrm{mm}$ for the VS150-M sensor and after the third drop from $850\,\mathrm{mm}$ for the VS 30-V sensor. The drop tests were stopped, when no wave-based signal was measurable, as the piezoelectric element inside the sensor became loose. The number of measurements and the corresponding drop heights for both sensors can be seen in Figure 1.

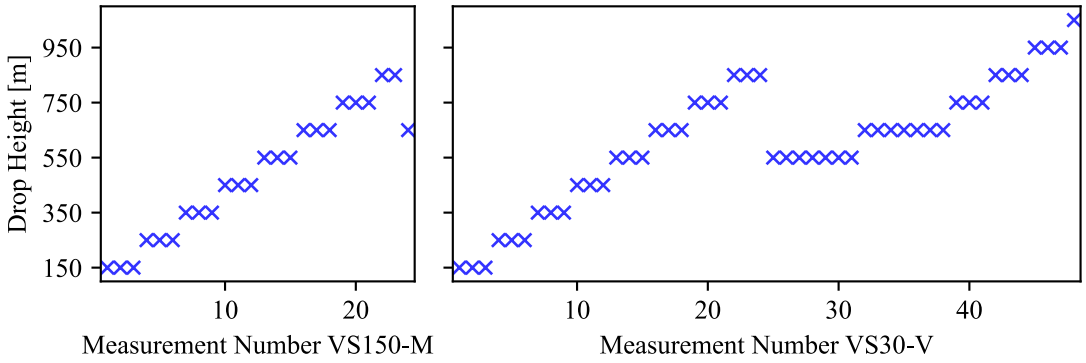


Figure 1. Drop heights for damaging the sensors VS150-M (left) and VS30-V (right).

The EMI spectrum of the AE sensor is recorded with a Bode100 vector network analyzer, performing a frequency sweep with an amplitude of less than $1\,\mathrm{V_{pp}}$ [13]. A measurement consists of 6401 data points of the impedance and admittance spectrum. For these, resistance as real part of impedance and susceptance as imaginary part of admittance are used for further evaluation. A linear distributed frequency range of $100\,\mathrm{kHz}$ to $450\,\mathrm{kHz}$ for the VS150-M sensor and $25\,\mathrm{kHz}$ to $80\,\mathrm{kHz}$ for the VS30-V sensor is used in the measurements. These frequency ranges correspond to the operating frequency ranges of the sensors [14].

To evaluate the condition of the sensor under test (SUT), nine features are extracted from the measured EMI spectrum and these features are compared with features extracted from EMI spectra of pristine sensors which are identical to the SUT. The following features are extracted from the resistance and susceptance spectra:

1. Two features: RMS of difference between a baseline and EMI spectra under test
2. Two features: CC between baseline and EMI spectra
3. Two features: RMS of deviation of first four/three (VS150-M/VS30-V) EFs

4. Two features: RMS of deviation of amplitudes of the EFs
5. One feature: Slope of linear section between first and second EF in susceptance spectrum

In order to perform the comparison, a baseline is built, a model is set up and the deviation from the model is determined.

Twelve sensors identical to SUT are measured in a pristine state with five measurements each. Twelve spectra — one of each sensor — are used to calculate an average baseline. For all other spectra, the features listed above are extracted using this baseline. To enable the comparison of one or two values summarizing all the nine features, a principal component analysis (PCA) model is built using 24 measurements — two of each sensor. The PCA is a statistical method that reduces data dimensionality while remaining data variability. It transforms correlated features into uncorrelated principal components (PCs). The model is limited to the first five PCs capturing over 97 % of the total variance. Before applying the PCA, the extracted features are standardized, mean-centered and scaled to unit variance [15]. This allows to extract Hotelling's $T^2$- and Q-statistic, which were employed as damage indices. The $T^2$-statistic quantifies variations within the PCA model. In contrast, the Q-statistic represents the residual error outside the used first five PCs. From the remaining 24 measurements, twelve — one of each sensor — are used as test data and to establish a threshold for $T^2$- and Q-statistic separately. Assuming a normal distribution, not proved using statistical test due to the small amount of available data, the threshold is set to the mean plus two times the standard deviation, resulting in approximately 97.5 %. The remaining twelve measurements — one for each sensor — are used as test data only.

Finally, the evaluation of the SUT is performed analog to the test data for all sensor states, resulting in $T^2$- and Q-statistic values for each measurement. It is expected that both values will exceed the threshold as soon as the SUT shows signs of damage.

The wave signal of the AE sensors is recorded as described in [5], with the sensor being coupled to a freely vibrating aluminum block, with a conical piezoelectric element on the opposite side. This element is utilized to generate elastic waves within the block by multiple $10\,\mathrm{V_{pp}}$ pulses with a pulsing frequency of $50\,\mathrm{Hz}$. The arriving elastic wave at the AE sensor is measured with a sampling rate of $40\,\mathrm{MHz}$ and at least 500 pulses were captured for one measurement. To assess the state of the sensor through feature extraction, the MATLAB-based software tool SENSORtoolbox was developed by the University of Augsburg [5]. It calculates the partial power for three different frequency ranges, the weighted peak-frequency and the amplitude of the signal. By comparing the measurement with a previously documented baseline, the significances of these calculations are determined and compared with a threshold. If one significance exceeds the threshold, the sensor gets classified as damaged. For the comparison of the drop test measurements, one single combined significance value is used. It is calculated as the sum of the normalized significances for the individual calculated partial powers, weighted peak-frequency and amplitude of the signal. For both methods, the cumulative drop height is used as a reference value.

## RESULTS

The occurring changes in the EMI spectrum and wave signal due to drop tests on the

AE sensor of the type VS30-V are exemplary illustrated in Figure 2. Measurements of the EMI of a baseline and two different damage states are displayed in Figure 2a) and b). The damage state 1 refers to the third drop from $850\,\mathrm{mm}$ (measurement no. 24) where the first larger deviation occurred in both measurements, EMI and wave-based without exceeding the significance level for the SENSORtoolbox criterium, while the damage state 2 stands for the fifth drop from $550\,\mathrm{mm}$ (measurement no. 26), where the sensor was classified as damaged from the SENSORtoolbox criterium. Figure 2c) and d) show the corresponding sensitivity spectra of the sensor measured with the wave-based setup for the two drop heights, respectively. In the EMI spectra, a reduction of the amplitude at approx. $57\,\mathrm{kHz}$ in the resistance spectrum as well as a shift into lower frequencies is noticeable as soon as damage occurs. Furthermore, the higher EF shows a larger frequency shift in the same direction. For the EF at approx. $54\,\mathrm{kHz}$ in the susceptance spectrum, the increasing amplitude and frequency shift remains the same for the two damage states. Nevertheless, the higher EF shows an increasing frequency shift towards lower frequency with increasing damage.

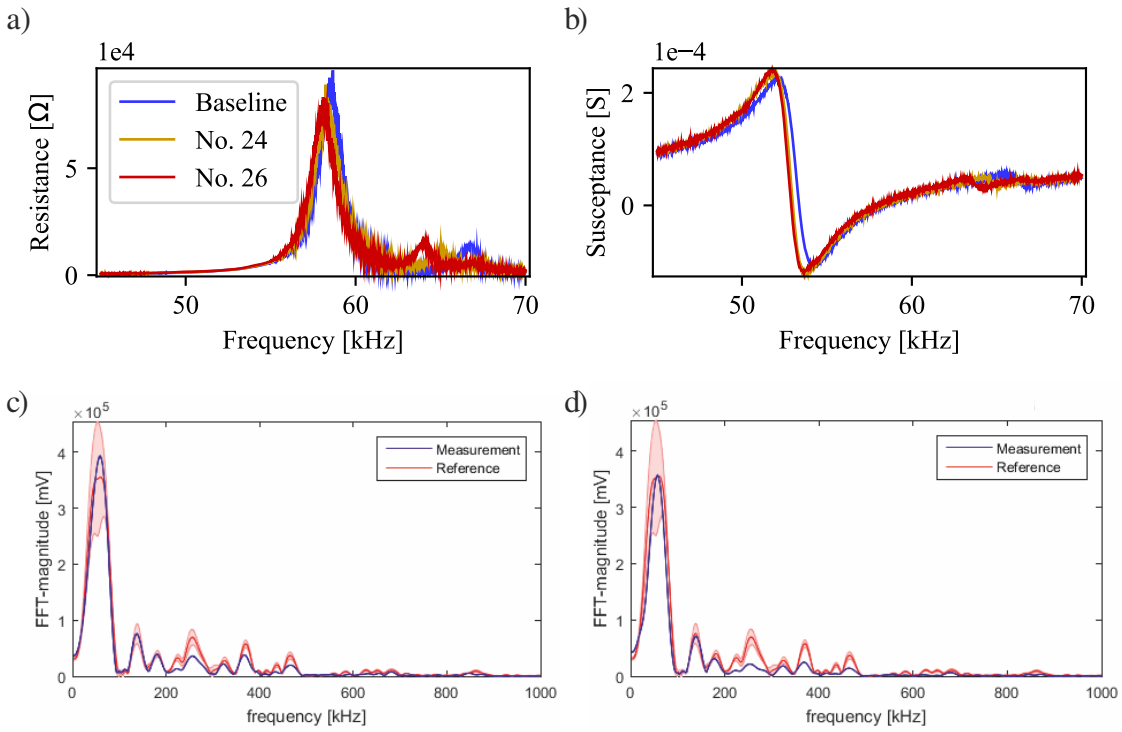


Figure 2. a) and b) EMI spectrum zoomed on second and third eigenfrequency: intact sensor (blue, baseline), measurement no. 24 after third drop $850\,\mathrm{mm}$ (orange), and measurement no. 26 after fifth drop from $550\,\mathrm{mm}$ (red). c) Sensitivity spectrum: intact (blue) vs. measurement no. 24 (red). d) Sensitivity spectrum: intact (blue) vs. measurement no. 26 (red).

The determined $T^2$- and Q-statistic values for the sensor types VS150-M and VS30-V are shown in Figure 3a) and c), respectively. In order to show the details of scattering for the undamaged state, a log-log scale is used. The calculated threshold is given by two red lines for the $T^2$- and Q-statistic. For the two sensors, Figure 3b) and d) show, the sum of the normalized significances calculated with the wave-based setup along with a red

line when the sensor was classified as damaged by the SENSORtoolbox. Considering the first sensor type VS150-M, shown in Figure 3a) and b), the training data (□) used for the PCA and the test data of the sensors identical to SUT (×) are grouped at low $T^2$- and Q-statistic values, with one train and test data point exceeding the threshold. Additionally, these values are also low for measurements of the SUT with a cumulative drop height below $11\,\mathrm{m}$. The corresponding significances of these measurements with the wave-based setup are also below 2. When the cumulative drop height exceeds $11\,\mathrm{m}$ (measurement no. 23) an increase in both damage indices of the PCA is noticeable. Furthermore, this behavior is observable within the wave-based measurements, although the criteria of a damaged sensor according to the SENSORtoolbox has not been met yet. Unfortunately, no measurement exists after the next drop height (cumulative drop height of $12\,\mathrm{m}$), as the piezoelectric element inside the sensor became loose and a verification to classify the sensor as damaged was not possible.

The $T^2$- and Q-statistic values of the PCA in Figure 3c) indicate a linear trend with increasing cumulative drop height beginning from $12\,\mathrm{m}$ until $17\,\mathrm{m}$ where both damage indices increase drastically for the sensor type VS30-V. The $T^2$- and Q-statistic values of the training (□) and testing data (×) used are low, except for two training and two intact data points. These points correspond to one specific sensor, that generally showed higher deviation in the EMI spectrum than the other sensors identical to SUT. For the significance calculated with the wave-based setup, a first increase is noticeable after the cumulative drop height of $12\,\mathrm{m}$. Two measurements with higher significance values without classifying the sensor as damaged are present. With the damaged classified sensor at $13\,\mathrm{m}$, a linear trend until $17\,\mathrm{m}$ is observable. These phenomena are also evident in the EMI measurements, which exhibit higher Q-statistic values compared to previous measurements and the intact sensor.

## DISCUSSION

With the features and variance limit chosen for the PCA, a differentiation between a defect and intact sensor is possible when using the $T^2$- and Q-statistic values. For the sensor type VS150-M only two measurements in a damaged state exist for the EMI. Therefore, gradual damage is not observable. The increase in the significance from the wave-based setup is also present in the PCA results, where both damage indices increase for the cumulative drop height of approx. $11\,\mathrm{m}$. As the piezoelectric element became loose in the sensor, it can be assumed, that a degradation of the adhesive layer between the element and the casing or wear plate, depending on the sensor's design, might be the type of damage. Hence, the last EMI measurement of the sensor results in a measurement of the piezoelectric element without any mechanical influences of the sensor's casing. The overall low $T^2$- and Q-statistic values for the training data and the intact sensor provide a reliable differentiation between the damaged and intact sensor. The fact that the data points of drop tests with lower cumulative drop heights (below $11\,\mathrm{m}$) are all in the region of the intact sensor is perfectly represented in the data of the reference setup (wave based), which likewise classifies these sensor states as intact with low significance values.

The determined $T^2$- and Q-statistic values within the PCA of the second sensor type VS30-V are low, especially for the Q-statistic, with all values being below 0.8. Within

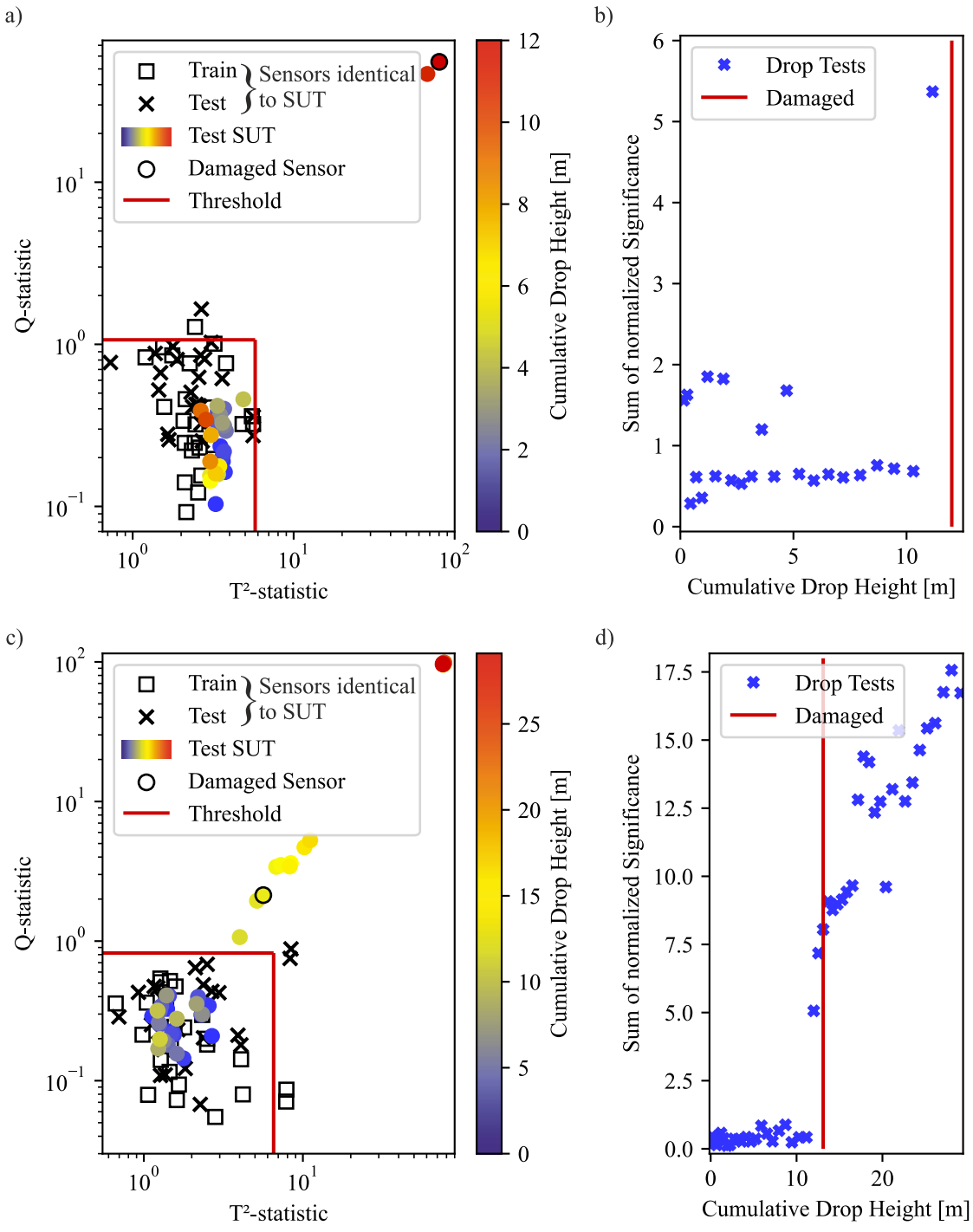


Figure 3. $T^2$- and Q-statistic values in log-log scale for training (□) and testing data (×) of sensors identical to SUT and drop test measurements (blue to red) shown on the left. The measurement classified as damaged by the wave-based setup is marked with a black circle and the calculated thresholds are given by red lines. Sum of normalized significance after the drop tests, calculated with the SENSORtoolbox given on the right; red line indicates wave-based damaged classification. a) and b) Sensor type VS150-M. c) and d) Sensor type VS30-V.

the $T^2$-statistic, the overall values are lower than 5, except for two training data points and two testing data points of one sensor identical to SUT that showed higher deviation in the EMI spectrum. As the $T^2$-statistic depicts the variation within the PC space, that was chosen to capture more than 97 % of the data variance, this occurring in the $T^2$-statistic is reasonable. Drop test measurements with a cumulative drop height below $12\,\mathrm{m}$ exhibit values for the $T^2$- and Q-statistic values as low as the training and intact data. Considering the evaluation by the wave-based setup, it can be seen that these measurements represent the sensor without being damaged. The deviation of the significances when increasing the cumulative drop height from $12\,\mathrm{m}$ to $17\,\mathrm{m}$ is also present as an increase in the $T^2$- and Q-statistic values, although the detection of the first damages is more reliable with the latter, as it is more distinguishable from the training and intact data. Detection of the defect sensor can be done with both damage indices, neglecting the one used sensor with overall higher deviations in the EMI spectrum and considering the mean plus two times standard deviation of all training and intact data.

## CONCLUSION

This study confirms the feasibility of using the EMI spectrum to detect mechanical damage in AE sensors. Controlled drop tests were used to systematically simulate realistic degradation scenarios. The extraction of defined features from the EMI spectrum enables the calculation of two damage indices using a PCA. The analysis of Hotelling's $T^2$- and the Q-statistic as damage indices, demonstrates a clear distinction between intact and defect sensors, as both damage indices remained low in undamaged states. Nevertheless, the Q-statistic provides more consistent differentiation during early-stage degradation for sensor type VS30-V. Applying statistical thresholds in both damage indices allows for robust defect identification. Validation against a wave-based verification setup, following the SE02 by the DGZfP [4] and conducted in cooperation with the University of Augsburg, demonstrates the reliability of the EMI-based approach. These results lay the basis for a self-diagnosis system capable of continuously monitoring AE sensor integrity directly in the field, minimizing the need for manual inspections and improving the reliability of long-term monitoring.

Future efforts should consider using the squared Mahalanobis distance to combine the $T^2$- and the Q-statistic into one damage index. Furthermore, a focus on expanding and validation EMI-based assessments for in-situ verification of AE sensors, as the results presented in this study are based exclusively on measurements obtained from freely vibrating AE sensors without structural attachment. To ensure broader applicability, it is essential to investigate how sensor installation, particularly the mechanical constraints introduced by bonding or mounting to a structure, affects the measurement results. In addition, future research should explore a wider range of sensor fault types, including those arising from thermo-mechanical loading, environmental aging, or long-term operational stress. Understanding how these factors affect the EMI spectrum will be crucial for developing a reliable and comprehensive self-diagnosis. Additionally, focusing on refining existing analytical models of the EMI spectrum of circular piezoelectric elements should be done to represent AE sensors in more detail. Therefore, the surrounding structure of the sensor's casing including the wear plate and the adhesive layer between the piezoelectric element and the casing needs to be considered. These advancements would not

only enhance model-based interpretation of EMI measurements but also support the development of robust, predictive self-monitoring systems for AE sensors under real-world conditions.

## REFERENCES


1. Grosse, C. U., M. Ohtsu, D. G. Aggelis, and T. Shiotani, eds. 2022. *Acoustic Emission Testing: Basics for Research – Applications in Engineering*, Springer Tracts in Civil Engineering, Springer International Publishing, Cham, ISBN 978-3-030-67935-4 978-3-030-67936-1, doi:10.1007/978-3-030-67936-1.
2. 2022, "Non-Destructive Testing - Acoustic Emission Testing - In-service Acoustic Emission Monitoring of Metallic Pressure Equipment and Structures - General Requirements; German Version EN 17391:2022," .
3. Vallen, H. 2023. "A New Iso Standard for AE Sensor Sensitivity Determination Uses the Face-to-Face Stimulation Method," *e-Journal of Nondestructive Testing*, 28(1), ISSN 14354934, doi:10.58286/27621.
4. DGZfP. 2014, "Guideline SE 02 - Verification of Sensors and Their Coupling in Laboratories." .
5. Sause, M. G., S. Schmitt, and P. Potstada. 2017. "Kontinuierliche Und Wiederkehrende Prüfung von Schallemissionssensoren," *21. Kolloquium Schallemission – Vortrag 24*.
6. Fernandes De Oliveira Junior, A., T. Schlech, and M. G. R. Sause. 2024. "Studies on a Mobile Acoustic Emission Sensor Verification Device," *e-Journal of Nondestructive Testing*, 29(10), ISSN 1435-4934, doi:10.58286/30240.
7. Buethe, I., B. Eckstein, and C.-P. Fritzen. 2014. "Model-Based Detection of Sensor Faults under Changing Temperature Conditions," *Structural Health Monitoring*, 13(2):109–119, ISSN 1475-9217, 1741-3168, doi:10.1177/1475921713510755.
8. Park, G. H., C. R. Farrar, A. C. Rutherford, and A. N. Robertson. 2004. "Piezo-Sensor Self-Diagnostics Using Electrical Impedance Measurements." Tech. Rep. LA-UR-04-7511, Los Alamos National Laboratory (LANL), Los Alamos, NM (United States).
9. Moix-Bonet, M., I. Buethe, M. Bach, C.-P. Fritzen, and P. Wierach. 2014. "Durability of Co-bonded Piezoelectric Transducers," *Procedia Technology*, 15:638–647, ISSN 22120173, doi:10.1016/j.protcy.2014.09.025.
10. Priebe, S., C. Reinhardt, A. Fernandes, H. Trattnig, M. G. R. Sause, and I. Mueller. 2024. "Electromechanical Impedance of Acoustic Emission Sensors Used for Self-Diagnosis," *e-Journal of Nondestructive Testing*, 29(7), ISSN 1435-4934, doi:10.58286/29632.
11. Reinhardt, C., S. Priebe, and I. Mueller. 2024. "The Influence of Coupling-Specific Parameters and Structural Parameters on the Electromechanical Impedance of Acoustic Emission Sensors," *e-Journal of Nondestructive Testing*, 29(10), ISSN 1435-4934, doi:10.58286/30268.
12. Reinhardt, C., S. Priebe, and I. Mueller. 2025. "Detection of Adhesive Layer Degradation in Acoustic Emission Sensors Using the Electromechanical Impedance for Self-Diagnosis," in *SCHALL 25 – Schallemissionsanalyse Und Zustandsüberwachung Mit Geführten Wellen, 27. – 28. März 2025, Dresden, Germany*, Deutsche Gesellschaft für Zerströgunsfreie Prüfung, Dresden, doi:10.58286/30965.
13. OMICRON Lab. 2024. *Technical Data Sheet Bode 100*, revision 2 edn.
14. Vallen. 2022. *Acoustic Emission Sensors and Preamplifiers - Specification*.
15. Mujica, L., J. Rodellar, A. Fernández, and A. Güemes. 2011. "Q-Statistic and T2-statistic PCA-based Measures for Damage Assessment in Structures," *Structural Health Monitoring*, 10(5):539–553, ISSN 1475-9217, 1741-3168, doi:10.1177/1475921710388972.